A Symmetry-Compatible Rhombus Mesh for Continuum Dislocation Dynamics Simulations in FCC Crystals

A. Kalaei [1*], D. J. Srolovitz[1], and A.H.W. Ngan[2]

[1] Department of Mechanical Engineering, The University of Hong Kong, Hong Kong, China

[2] School of Metallurgy and Materials, University of Birmingham, Birmingham, United Kingdom

* *Corresponding author (akalaei@connect.hku.hk)*

Keywords: *Dislocation dynamics; Crystal plasticity; FCC crystal; Finite difference method*

1. Abstract

The "all-dislocation" density (ADD) dynamics model is a continuum dislocation dynamics (CDD) framework for simulating plastic deformation by tracking the collective motion of dislocations. ADD can simulate plasticity while the individual dislocation lines are smeared out over hundreds of Burgers vectors yet still capture the influence of statistically stored dislocations (SSDs) on both short- and long-range interactions. The original formulation, which has been successfully published, employed a Finite Difference Method (FDM) on an orthogonal mesh to solve the kinematic ADD equations numerically. However, the geometry of an orthogonal mesh is not compatible with the inherent symmetry of face-centred cubic (FCC) slip systems. This mismatch requires interpolation for the computation of dislocation interactions and for the treatment of mechanisms such as cross-slip, which may reduce the accuracy of critical plasticity processes.
In this work, we present an advancement of the ADD model through the development and implementation of an FCC-compatible rhombus mesh structure. This mesh, with internal angles of $\pi/3$ and $2\pi/3$, is compatible with FCC crystallography and allows slip-plane intersections to be represented directly by the mesh. As a result, short-range interactions can be computed while avoiding interpolation-related artifacts. Furthermore, the symmetry-compatible structure provides a natural framework for the simulation of cross-slip.

The proposed numerical model is applied to simulate dislocation loop expansion under a constant velocity field to provide an initial verification of the formulation and to demonstrate its potential for future applications to 3D dislocation microstructure simulations.

2. Introduction

Dislocation plasticity models have been widely used for the simulation of the mechanical behaviour of metal matrix composites [1]-[4]. These models range from atomistic simulations [1] such as Molecular Dynamics (MD), to mesoscopic crystal plasticity models such as discrete dislocation dynamics (DDD) [4],

[5] and Continuum Dislocation Dynamics (CDD) [3], up to macroscopic crystal plasticity (CP) models [2]. Models with higher fidelity usually suffer from high computational cost, while coarser models may ignore critical physics of plasticity.

CDD models lie between DDD and CP by coarse-graining dislocations into density fields [6]-[9]. The "all-dislocation" density (ADD) dynamics model is one of the CDD frameworks capable of simulating plasticity over a wide range of dislocation densities by tracking the evolution of the ADD density, $\varrho(\vec{r},\theta)$ [6, 10]. This framework can track the evolution of geometrically necessary dislocations (GNDs) and statistically stored dislocations (SSDs) simultaneously, unlike many other CDD models [9, 11]. The kinematic evolution law for ADD was previously solved numerically using an orthogonal rhombus mesh structure, as presented by Kalaei et al [6]. This rhombus mesh structure was used to simulate plasticity in 3D FCC crystals. For short-range dislocation interactions, a cut-off radius was introduced within which dislocations from different slip systems interact. However, this mesh structure does not consider the symmetry of FCC and requires searching for neighboring nodes for every node when computing short-range interactions, which is computationally expensive and may reduce accuracy. Furthermore, since slip-plane intersections are not explicitly represented in this structure, the simulation of cross-slip is not feasible.

Here, we show that the mesh structure formed by the traces of slip-plane intersections on a given slip plane in FCC crystals contains angles of $\pi/3$ and $2\pi/3$. Every node in this structure carries the density contributions of more than one slip plane. Based on this geometry, we modify the orthogonal rhombus mesh structure of Kalaei et al. [6] to obtain a new FCC-compatible mesh structure. In addition, dislocation loop expansion under constant velocity is simulated to provide an initial verification of the developed numerical scheme.

3. "All-dislocation" density dynamics (ADD)

ADD is a mesoscopic plasticity model that provides a kinematically exact evolution law for $\rho(\vec{r},\theta)$, a dislocation density representation defined in terms of spatial position and orientation. Ngan [10] showed that the evolution law for $\rho(\vec{r},\theta)$, composed of a glide and rotation term can be written as

$$\dot{\rho}_\alpha(\vec{r},\theta) = -\left(\frac{\partial(\rho_\alpha v_\alpha)}{\partial \hat{r}_\theta}\right)_{glide} - \left(\frac{\partial(\rho_\alpha \omega_\alpha)}{\partial \theta}\right)_{rotation} \quad (1)$$

where α, v_α, $\hat{r}_\theta$, and ω_α denote, respectively, the slip plane on which the dislocations glide, the velocity field, the direction normal to the dislocations, and the rotational velocity of the dislocations arising from velocity gradients, given by

$$\omega_\alpha(\vec{r}) = \frac{\partial v_\alpha(\vec{r},\theta)}{\partial \hat{\xi}_\theta}. \quad (2)$$

Here, $\hat{\xi}_\theta$ denotes the tangent direction to the dislocation line. This equation defines the rotational velocity of a dislocation line as the gradient of the velocity along the tangent direction of the dislocation. The velocity $v_\alpha$must, in general, be determined from dislocation interactions.

However, the treatment of dislocation interactions for determining the velocity field is beyond the scope of the present work.

4. FCC-compatible mesh structure

In previous work, a rhombus mesh structure was introduced to solve Eq. 1. In particular, Kalaei et al. [6] used an orthogonal rhombus mesh where the element side lengths were identical. In this work, we extend the framework to a non-uniform mesh structure. This mesh is composed of rhombuses with internal angles of π/3 and 2π/3, a geometry that is more compatible with the crystallographic symmetry of FCC crystals. Specifically, this rhombus mesh structure is formed by the intersection of slip planes on one of the primary slip planes (see Fig. 1a). Because the nodes are located exactly at these intersections, each node inherently contains the information of several slip planes. As a result, this geometry reduces the need to apply interpolation when computing short-range interactions and model cross-slip.

Let points A, B, C, and D be the corners of a quadrilateral mesh element where the dislocation flux is computed (see Fig. 1b). Following the approach of Kalaei et al. [6], an expression can be written for the rate of change of the mobile dislocation density, $\dot{\rho}^{\text{move}}(\theta)$, within the element ABCD. The flux balance equations for the parallel sides AB and CD are given as follows:

$$\dot{\varrho}^{move}(\theta)|_{ABCD}\,\overrightarrow{AB}\cos\left(\theta_{\overrightarrow{AB}}-\theta_v\right)=-\Delta(\varrho v_\theta)|_{\overrightarrow{AB}} \tag{3}$$

$$\dot{\varrho}^{move}(\theta)|_{ABCD}\,\overrightarrow{CD}\cos\left(\theta_{\overrightarrow{CD}}-\theta_v\right)=-\Delta(\varrho v_\theta)|_{\overrightarrow{CD}} \tag{4}$$

Here, we consider a case where the length of segment CD is $\sqrt{3}$ times the length of segment AB (i.e., $|\overrightarrow{CD}|=\sqrt{3}\,|\overrightarrow{AB}|$). If we define the length of segment AB as Δs, and combine Eqs. 3 and 4, the result for the dislocation density rate at a node $(i,j)$is:

$$\dot{\varrho}^{move}(\theta)|_{i,j}\,\Delta s=-\left[\Delta\left(\varrho v(\theta)\right)\big|_{\overrightarrow{AB}}\,\hat{s}+\frac{\Delta(\varrho v(\theta))|_{\overrightarrow{CD}}}{\sqrt{3}}\hat{e}\right]\cdot\hat{\theta} \tag{5}$$

In Eq. 5, $\hat{s}$ and $\hat{e}$ are unit vectors representing the screw and edge dislocation directions, respectively, and $\hat{\theta}$ is the unit tangent vector of the dislocation line. The dislocation density and velocity at the element nodes (A, B, C, and D) are obtained by interpolating from the surrounding grid points: (i,j), $(i+1,j)$, $(i,j+1)$, $(i-1,j)$, and $(i,j-1)$.

We have also developed a numerical method for simulating the interaction between dislocation lines and grain boundaries (GBs). In this method, the dislocation density flux at the GB nodes is replaced by an equation that computes the inter-granular dislocation density flux, denoted as $J(\vec{r},\theta)$.

For this formulation, the simulation domain consists of rhombus-shaped elements with internal angles of $\pi/3$ and $2\pi/3$. We consider a scenario, depicted in Fig. 1b, where a grain boundary is present such that nodes B and D of a mesh element lie on the GB. Consequently, the dislocation

flux at these nodes is assumed to be zero: $(\rho v(\theta))_B = 0$ and $(\rho v(\theta))_D = 0$. Applying this boundary condition to the discretization scheme and incorporating the inter-granular flux term J, Eq. 5 is modified for a node (i, j) on the boundary as follows:

$$\dot{\varrho}^{move}(\vec{r},\theta)|_{i,j}\,\Delta s = -\left[-\left(\varrho v(\vec{r},\theta)\right)_A \hat{s} - \frac{\left(\varrho v(\vec{r},\theta)\right)_C}{\sqrt{3}}\hat{e}\right]\cdot\hat{\theta} + J(\vec{r},\theta) \tag{6}$$

It is important to note that Eqs. 5 and 6 govern the glide term in Eq. 1. The rotation of dislocation lines can be simulated using the approach proposed by Kalaei et al. [6], which involves computing the velocity gradient and projecting it onto the tangent direction of the dislocation. Additionally, a fourth-order Runge-Kutta method can be employed for the time integration.

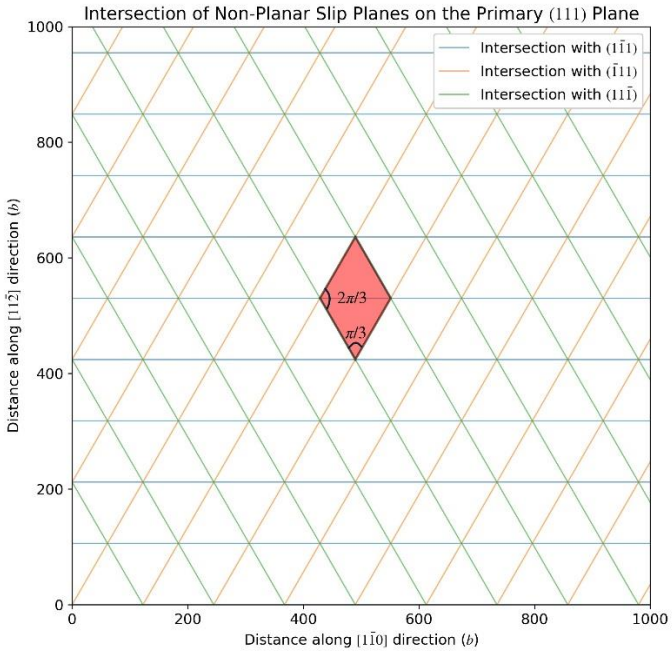

(a)

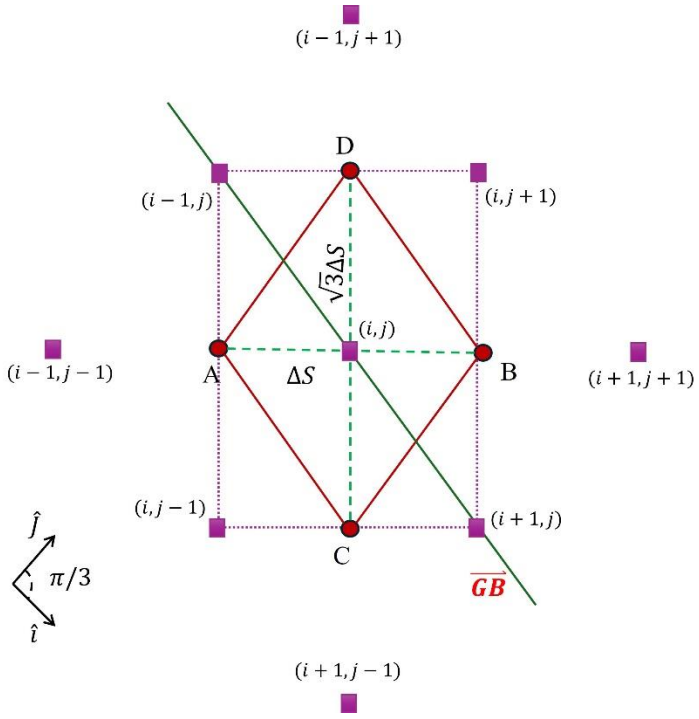

(b)

Figure 1. Schematic of the rhombus mesh structure compatible with the symmetry of FCC crystals. (a) Intersections between the primary (111) slip plane and other non-coplanar slip planes, showing the resulting mesh structure formed by the traces of these intersections. The parallel distance between intersecting slip planes is $500b$. (b) The computational stencil on the FCC symmetry-compatible mesh and the node structure at a grain boundary. Dislocation density flux is computed at the circled points via interpolation from the primary grid points. The line labeled $\overrightarrow{GB}$ represents the location of the grain boundary, where nodes B and D lie on the boundary, while nodes A and C are located inside the grain.

5. Dislocation loop expansion simulation

In the previous section, an FCC-compatible mesh structure was introduced for the simulation of ADD. To provide an initial verification of this numerical framework, the expansion of a dislocation loop under a constant velocity field is simulated. It should be emphasized that the numerical scheme presented in Eqs. 5 and 6 is designed for coarse-grained ADD. Consequently, the modeled dislocation loop represents a coarse-grained approximation rather than a discrete dislocation with exact physical dimensions.

For this simulation, Eq. 5 is used to model the loop expansion for nodes within the interior of the domain, while Eq. 6 is applied to the boundary nodes. The simulation assumes impenetrable boundary conditions; therefore, the inter-granular flux term, J, in Eq. 6 is set to zero. Dislocation segment interactions are neglected in this setup, and a uniform velocity corresponding to $1b$ per

time step is applied across the entire domain. The mesh size is set to 4b, the domain size to 600b, and the numerical profile width of the dislocation lines to 5b.

Figure 2d illustrates a linear relationship between the dislocation density and time. Given the constant velocity field, this linear growth is physically expected, thereby providing initial verification of the proposed numerical scheme. Furthermore, Figs. 2a through 2c depict the spatial expansion of the dislocation line over time. Together, these results confirm the applicability of this numerical model for simulating mesoscopic plasticity in FCC crystals.

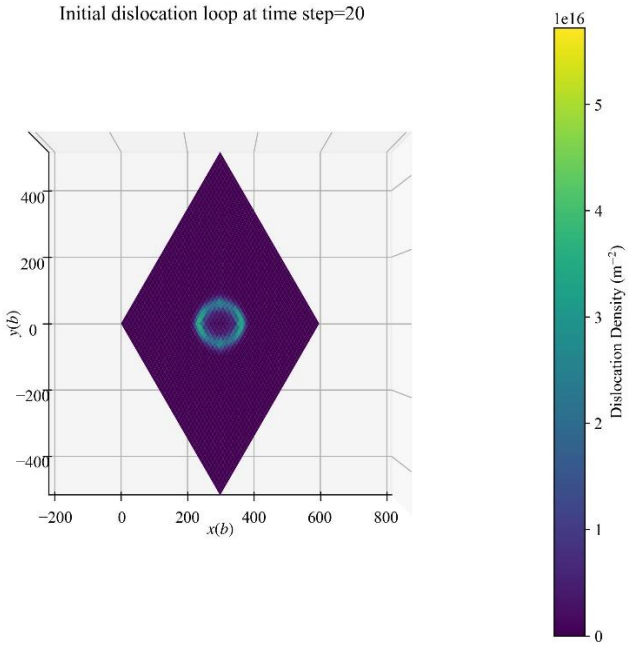

(a)

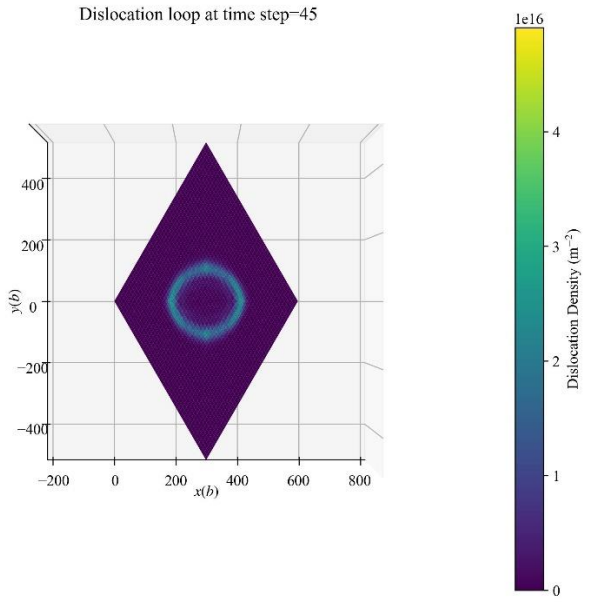
Dislocation loop at time step=45
1e16
4
3
2
1
0
Dislocation Density (m⁻²)
400
200
0
−200
−400
y(b)
−200
0
200
400
600
800
x(b)

(b)

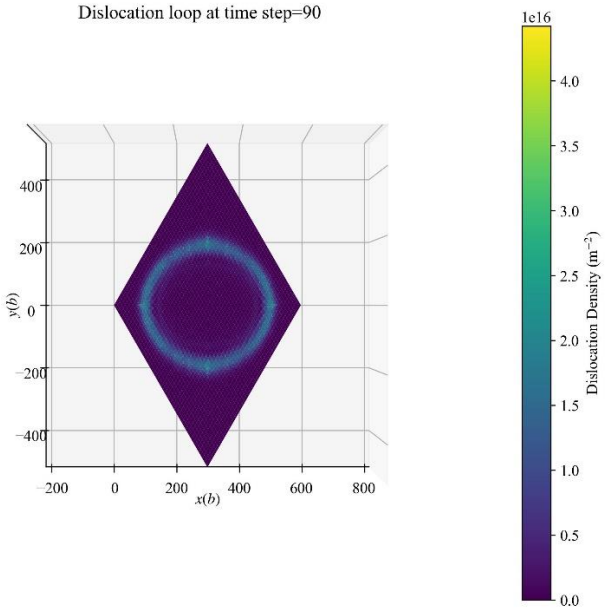
Dislocation loop at time step=90
1e16
4.0
3.5
3.0
2.5
2.0
1.5
1.0
0.5
0.0
Dislocation Density (m⁻²)
400
200
0
−200
−400
y(b)
−200
0
200
400
600
800
x(b)

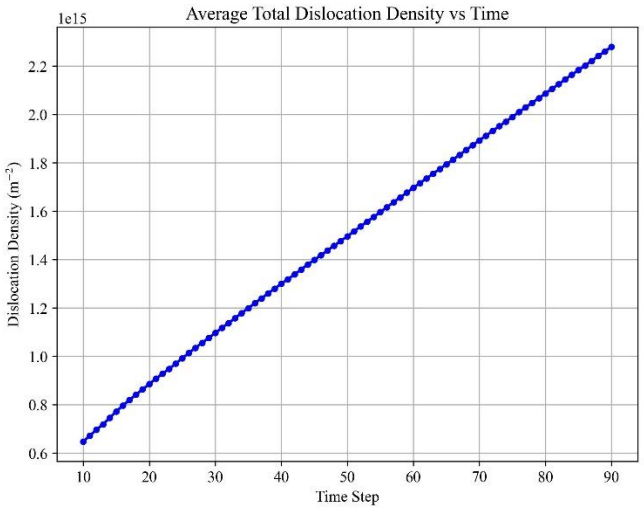

(d)

Figure 2. Simulation of loop expansion under a constant velocity field. Eqs. 5 and 6 are used to simulate loop expansion on an FCC-compatible rhombus mesh structure.

6. Conclusion

For the simulation of plasticity using Continuum Dislocation Dynamics (CDD), it is necessary to apply a mesh structure that is compatible with the symmetry of the simulated crystals in order to minimize numerical artifacts and inaccuracies. It is demonstrated that the symmetry-compatible mesh for FCC crystals is a rhombus mesh with internal angles of $\pi/3$ and $2\pi/3$. An FDM approach is employed to numerically solve ADD, a type of CDD model. As an initial verification of the proposed rhombus FDM, a dislocation loop expansion under a constant velocity field is simulated.

The current numerical method requires further development for multiple-slip-system plasticity simulations, where forest hardening and the short-range interaction of dislocations play a crucial role. Additionally, it is necessary to incorporate dislocation interactions into this framework, which will enable the simulation of stress-driven cross-slip of screw dislocations.

7. References

[1] C. Xing, J. Sheng, L. Wang, and W. Fei, “Research progress in molecular dynamics simulation of CNT and graphene reinforced metal matrix composites,” *Oxford Open Materials Science*, vol. 1, no. 1, p. itab008, Jan. 2021, doi: 10.1093/oxfmat/itab008.

[2] L. Tian, A. Russell, and I. Anderson, “A dislocation-based, strain–gradient–plasticity strengthening model for deformation processed metal–metal composites,” *J. Mater. Sci.*, vol. 49, no. 7, pp. 2787–2794, 2014.

[3] K. Schulz, M. Sudmanns, and P. Gumbsch, "Dislocation-density based description of the deformation of a composite material," *Model. Simul. Mat. Sci. Eng.*, vol. 25, no. 6, p. 064003, 2017.

[4] S. S. Shishvan, R. M. McMeeking, T. M. Pollock, and V. S. Deshpande, "Discrete dislocation plasticity analysis of the high-temperature cyclic response of composites," *Materials Science and Engineering: A*, vol. 712, pp. 714–719, Jan. 2018, doi: 10.1016/J.MSEA.2017.12.034.

[5] H. H. M. Cleveringa, E. Van Der Giessen, and A. Needleman, "Comparison of discrete dislocation and continuum plasticity predictions for a composite material," *Acta Mater.*, vol. 45, no. 8, pp. 3163–3179, Aug. 1997, doi: 10.1016/S1359-6454(97)00011-6.

[6] A. Kalaei, Y. Xiang, and A. H. W. Ngan, "An efficient and minimalist scheme for continuum dislocation dynamics," *Int. J. Plast.*, vol. 158, p. 103433, Nov. 2022, doi: 10.1016/j.ijplas.2022.103433.

[7] A. Kalaei, J. Yu, J. Han, D. J. Srolovitz, and A. H. W. Ngan, "A flux boundary condition for grain boundary-dislocation interaction using all-dislocation density dynamics (ADD)," *Int. J. Plast.*, vol. 196, p. 104554, 2026.

[8] P. Lin and A. El-Azab, "Implementation of annihilation and junction reactions in vector density-based continuum dislocation dynamics," *Model. Simul. Mat. Sci. Eng.*, vol. 28, no. 4, p. 045003, 2020.

[9] A. Acharya and A. Roy, "Size effects and idealized dislocation microstructure at small scales: predictions of a phenomenological model of mesoscopic field dislocation mechanics: Part I," *J. Mech. Phys. Solids*, vol. 54, no. 8, pp. 1687–1710, 2006.

[10] A. H. W. Ngan, "Dislocation-density kinematics: a simple evolution equation for dislocation density involving movement and tilting of dislocations," *MRS Commun.*, vol. 7, no. 3, pp. 583–590, 2017.

[11] T. Hochrainer, M. Zaiser, and P. Gumbsch, "Dislocation transport and line length increase in averaged descriptions of dislocations," in *AIP Conference Proceedings*, American Institute of Physics, 2009, pp. 1133–1136.